Improved equation of state for the classical one-component plasma

W. L. Slattery and G. D. Doolen

Los Alamos Scientific Laboratory, Theoretical & Theoretical Design Divisions, Los Alamos, New Mexico 87545

H. E. DeWitt

Lawrence Livermore Laboratory, Livermore, California 94550

We compute the internal energy of the classical one-component plasma, for values of the Coulomb coupling parameter Γ between 1 and 300, by using converged Monte Carlo chains and a more accurate potential approximation than that used by Hansen. The liquid data are fitted to a simple, very accurate four-parameter formula from which the Helmholtz free energy is derived. The solid data are likewise fitted to a one-parameter formula. The intersection of the two free-energy curves gives an estimate of the fluid-solid transition at $\Gamma = 168 \pm 4$.

I. INTRODUCTION

The classical one-component plasma (OCP) is an idealized system of ions immersed in a uniform sea of electrons such that the whole system is electrically neutral. This system is characterized by the Coulomb coupling parameter Γ, where $\Gamma = (Ze)^2/\bar{r}kT$ with the ion sphere radius $\bar{r} = (4\pi N/3V)^{-1/3}$, N the number of ions and V is the volume of the system.

Following the pioneering Monte Carlo work of Brush, Sahlin, and Teller[1] (hereafter BST) on the OCP, Hansen[2] dramatically improved the accuracy of the equation of state by improving the approximation of the interparticle potential and by using long Monte Carlo runs. However, DeWitt[3] has questioned the accuracy of Hansen's data for large values of the Coulomb coupling parameter $(40 < \Gamma < 160)$. DeWitt thought that the reduced precision for large Γ may have been due to Monte Carlo noise or to possible systematic errors. In this paper we report the results of calculations similar to but more accurate than the results of Hansen and Brush, Sahlin and Teller. Systematic deviations from Hansen's results are found and our estimation for the fluid-solid transition is $\Gamma = 168 \pm 4$.

For the potential approximation used here the error in evaluating the Madelung sum is of order 1 part in 10^6. This compared with an error of order 1 part in 10^3 for Hansen's approximation. We also extend the range of the pair distribution functions by including in the averages, particles in the volume $(V = L^3)$ inside the basic periodic cube but outside the inscribed sphere with radius $L/2$.

In Sec. II we discuss the various approximations to the Ewald potential (Hansen,[1] and DeWitt and Hubbard[4]). It is shown that our approximation to the potential is at least two orders of magnitude

more accurate than Hansen's. The fit to the potential which we used (cubic harmonics specialized for a vector computer) is described in detail in Appendix A. The data and a simple very accurate four-parameter fit to the liquid data, and a one-parameter fit to the solid data are discussed in Sec. III. Appendix B gives analytic formulas for normalizing the extended pair distribution function.

II. INTERPARTICLE POTENTIAL APPROXIMATION

Following BST, the total internal energy of a system U may be written

$$\frac{U}{NkT} = \frac{U_0}{NkT} + \frac{1}{2} \sum_{i \neq j = 1}^{N} \frac{\psi}{NkT}(|\vec{r}_i - \vec{r}_j|), \tag{1}$$

where

$$\frac{\psi}{NkT} = \frac{\Gamma}{NL}[U_1(r) + U_2(\vec{r})], \tag{2}$$

and

$$U_1(r) = (1/r)\text{erfc}(\pi^{1/2}r) - 1, \tag{3}$$

$$U_2(\vec{r}) = \sum_{\vec{n}}{}' \frac{1}{|\vec{n} - \vec{r}|}\text{erfc}(\pi^{1/2}|\vec{n} - \vec{r}|)$$

$$+ \sum_{\vec{n}}{}' \frac{1}{\pi n^2}\exp(-\pi n^2)\{\exp[i(2\pi\vec{n} \cdot \vec{r})]\}. \tag{4}$$

Here the interparticle separation $\vec{r} = \vec{r}_i - \vec{r}_j$ is in units of L where $L = (4\pi N/3)^{1/3}$ in units of the ion sphere radius $\bar{r}$ with N the number of particles.

In these units the minimum and maximum values for any component of r are 0 and 1, respectively, inside the basic periodic cube. $\vec{n}$ is a vector with integer components and the prime on the summations indicates that the zero $\vec{n}$ vector $(0, 0, 0)$ is to be excluded. In terms of the above,

$$\frac{U_0}{NkT} = \frac{\Gamma}{2L}[U_2(0) - 3] = -\frac{\Gamma}{2L}E_m,$$

TABLE I. Errors in potential approximations (all errors are relative).

Error description	Polynomial used here	DeWitt and Hubbard (Ref. 4)	Hansen (Ref. 2)
rms	4.9×10^{-8}	4.2×10^{-7}	1.4×10^{-5}
average (indicates amount of cancellation for a uniform distribution)	6.5×10^{-8}	-2.0×10^{-5}	-4.0×10^{-4}
maximum	2.1×10^{-4}	3.9×10^{-4}	1.1×10^{-2}

or $E_m = 3 - U_2(0)$ where $E_m = 2.837\,297\,479$ is the Madelung energy of a simple cubic crystal with lattice spacing L. Since Eq. (4) is difficult to compute rapidly it is customary to approximate it in some other form. BST used a Taylor expansion, Hansen[2] used what he called an "optimized Kubic harmonic" expansion, and DeWitt and Hubbard[4] used a 3D table look-up and interpolation. Since we are using a vector computer which evaluates polynomials rapidly we shall use ordinary cubic harmonics such as those used by Slater and DeCicco.[5] We describe this approach in detail in Appendix A.

We now show that our potential approximation is several orders of magnitude more accurate than previous calculations. To evaluate the errors in the various potential approximations we computed the potential at 64 000 random points to within a few parts in 10^{10} using Eq. (4). This value was then compared with the values of Hansen, DeWitt, and Hubbard and our polynomial values. The results are shown in Table I for 64 000 random points. As noted by Hansen, ordinary cubic harmonics converge poorly for $r > L/2$ but this error may be decreased by taking enough terms. The cubic harmonic approximation places the largest relative error where the potential is the smallest. This is in contrast with Hansen's optimized Kubic harmonics which place the largest error where the potential contributes much more to the total sum. The errors in the DeWitt and Hubbard scheme are distributed more uniformly since it is a table look-up and interpolation procedure. Their method could be made more accurate but table look-up is a relatively slow procedure on a vector machine. To estimate the systematic errors of the various potentials we placed the particles in a bcc (128 ions) or fcc (108 ions) lattice and evaluated the static internal energy. The resulting static energy may be compared directly with the Madelung energy of that lattice. The results show that for the potential used here the systematic errors are of order 1 part in 10^6 whereas Hansen's potential has systematic errors of order 1 part in 10^3. With the polynomial potential the errors de-

crease with increasing numbers of ions, for example, bcc lattices with 432 and 686 ions have systematic errors of 4 parts and 1 part in 10^7, respectively.

By rearranging the Ewald sum we were able to write a computer code that was about three times faster than the polynomial code, but it was not used because it was one-half order of magnitude less accurate.

III. RESULTS AND DISCUSSION

Table II gives the internal energies (U/NkT), corrected for center-of-mass motion, for our calculations on the one-component plasma. The number of configurations in the Monte Carlo (MC) chains varied from 10^6 (with 10^5 previously discarded) for the lower Γ on up to 8.6×10^6 (with 0.2×10^6 to 1.5×10^6 previously discarded) for the higher Γ. Most of the calculations were done using 128 particles; a few 54, 108, 250, and 432 particle calculations were also done. The "lattice" after some of the entries indicates that a bcc or fcc lattice start was used. The statistical errors σ are the standard deviations of the means. These errors were computed after ensuring that there was negligible slope in the internal energy data.

Comparison of the data for the 128 ions and 250 ions shows a dependence on the numbers of ions (N dependence). As expected this N dependence is not nearly as strong when comparing the 250 data with the 432 data. Apparently a few hundred particles are necessary for the N-dependence errors to be negligible. Consequently the results in this paper which are all based upon the $N = 128$ runs are subject to a small systematic error. For $\Gamma = 180$ the random start was seen to solidify after 1.6×10^6 configurations. Figure 1 shows the pair distribution functions for the liquid (dashed curve) and solid (solid curve). All lattice starts with $\Gamma < 160$ melted and all random starts with $\Gamma \geq 170$ solidified. For calculation of structure factors, we give various pair distribution functions in Table III.

The systematic deviations of Hansen's[2] data from

TABLE II. Internal energies. U/NkT is the excess internal energy per ion divided by kT. We give our results and those of Hansen (Ref. 2) and Pollock and Hansen (Ref. 10).

Γ	U/NkT	Error $(\pm\sigma)$	Number of ions N	Type of start	U/NkT (Refs. 2 and 10)
1.0	−0.573	0.000	108	liq[a]	
1.0	−0.573	0.000	128	liq	−0.580
2.0	−1.320	0.001	128	liq	−1.318
3.0	−2.112	0.001	128	liq	−2.111
4.0	−2.927	0.001	128	liq	−2.926
6.0	−4.592	0.001	108	liq	
6.0	−4.593	0.001	128	liq	−4.590
10.0	−7.993	0.001	108	liq	
10.0	−7.992	0.002	128	liq	−7.996
15.0	−12.310	0.002	108	liq	
15.0	−12.309	0.003	128	liq	−12.313
20.0	−16.668	0.004	128	liq	−16.667
30.0	−25.426	0.004	108	liq	
30.0	−25.431	0.004	128	liq	−25.429
40.0	−34.251	0.004	108	liq	
40.0	−34.248	0.002	128	liq	−34.232
60.0	−51.941	0.006	54	liq	
60.0	−51.961	0.006	108	liq	
60.0	−51.961	0.007	128	liq	−51.936
80.0	−69.714	0.006	54	liq	
80.0	−69.727	0.005	108	liq	
80.0	−69.715	0.005	128	liq	−69.690
100.0	−87.511	0.007	54	liq	
100.0	−87.534	0.004	108	liq	
100.0	−87.500	0.005	128	liq	−87.480
100.0	−87.498	0.005	250	liq	
110.0	−96.411	0.005	128	liq	−96.360
125.0	−109.825	0.007	108	liq	
125.0	−109.780	0.004	128	liq	−109.732
125.0	−109.793	0.005	250	liq	
125.0	−109.799	0.004	432	liq	
140.0	−123.239	0.010	108	liq	
140.0	−123.160	0.006	128	liq	−123.095
140.0	−123.165	0.007	250	liq	
150.0	−132.078	0.007	128	liq	
160.0	−141.098	0.009	108	liq	
160.0	−141.000	0.006	128	liq	−140.890
160.0	−141.051	0.007	432	liq	
160.0	−141.690	0.010	108	lat[b]	
160.0	−141.729	0.006	128	lat	−141.717
160.0	−141.716	0.009	250	lat	
170.0	−150.703	0.005	128	lat	−150.696
180.0	−159.654	0.007	108	lat	
180.0	−159.675	0.004	128	lat	−159.662
180.0	−159.669	0.005	250	lat	
180.0	−159.667	0.004	432	lat	
200.0	−177.574	0.005	108	lat	
200.0	−177.619	0.004	128	lat	−177.604
220.0	−195.551	0.006	128	lat	−195.538
240.0	−213.469	0.003	128	lat	−213.470
300.0	−267.205	0.008	108	lat	
300.0	−266.675	0.006	125	lat	
300.0	−267.243	0.004	128	lat	−267.242

[a] liq denotes liquid.
[b] lat denotes lattice.
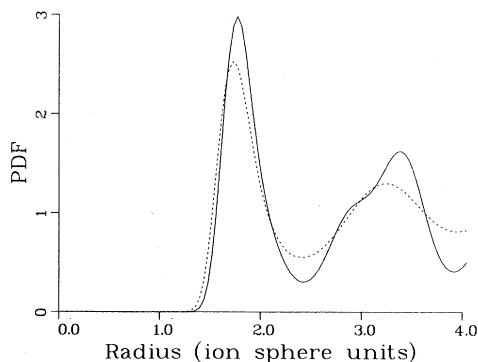
FIG. 1. Pair distribution functions for the liquid (dashed curve) and the solid (solid curve) for $\Gamma = 180$.

our data can be seen more clearly in Fig. 2 where we have plotted the thermal fraction of the internal energy, $(U - U_0)/NkT$, for our data (solid curve) and Hansen's[2] data, and the data of Pollock and Hansen[10] (dashed curve). Since Hansen's statistical errors are larger than ours by a factor of order 2, the differences can mostly be attributed to the fact that our potential is two to three orders of magnitude more accurate than Hansen's.

The liquid U/NkT data ($1 \leq \Gamma \leq 160$) for 128-particle runs were fitted to the form

$$U/NkT = a\Gamma + b\Gamma^{1/4} + c\Gamma^{-1/4} + d, \tag{5}$$

by minimizing the sum of the squares of the relative errors using a, b, c, and d as parameters. The fitted U/NkT are shown in Table IV along with

TABLE III. Pair distributions as a function of Γ and radius (ion sphere units).

Γ	80	110	125	140	150	160
Radius						
0.0406	0.000 00	0.000 00	0.000 00	0.000 00	0.000 00	0.000 00
to						
0.9343	0.000 00	0.000 00	0.000 00	0.000 00	0.000 00	0.000 00
1.0155	0.000 09	0.000 00	0.000 00	0.000 00	0.000 00	0.000 00
1.0967	0.001 22	0.000 07	0.000 00	0.000 00	0.000 00	0.000 00
1.1780	0.014 07	0.002 76	0.001 22	0.000 48	0.000 29	0.000 17
1.2592	0.084 93	0.029 62	0.015 89	0.009 57	0.006 45	0.004 63
1.3404	0.301 61	0.161 45	0.116 79	0.085 86	0.066 37	0.053 93
1.4217	0.710 33	0.526 91	0.447 56	0.377 14	0.328 13	0.295 71
1.5029	1.232 54	1.115 59	1.053 75	0.990 15	0.926 28	0.892 07
1.5842	1.674 27	1.719 58	1.714 91	1.714 90	1.701 76	1.689 81
1.6654	1.893 91	2.066 66	2.135 04	2.194 21	2.245 00	2.267 08
1.7466	1.880 92	2.084 05	2.180 90	2.259 57	2.331 61	2.378 48
1.8279	1.708 98	1.871 24	1.946 83	2.012 67	2.076 37	2.117 11
1.9091	1.479 63	1.568 49	1.615 10	1.650 84	1.683 86	1.708 76
1.9904	1.250 13	1.278 67	1.294 15	1.307 14	1.312 53	1.323 01
2.0716	1.060 53	1.046 32	1.040 28	1.035 00	1.025 50	1.020 30
2.1528	0.917 31	0.879 93	0.858 78	0.841 11	0.826 94	0.816 29
2.2341	0.814 72	0.765 61	0.735 94	0.718 28	0.699 34	0.682 62
2.3153	0.750 79	0.694 99	0.667 14	0.647 50	0.625 69	0.606 64
2.3966	0.720 72	0.664 16	0.638 59	0.614 36	0.593 26	0.579 68
2.4778	0.715 86	0.664 07	0.639 73	0.617 45	0.596 13	0.586 18
2.5590	0.738 45	0.688 53	0.666 43	0.647 85	0.629 29	0.624 30
2.6403	0.778 04	0.734 26	0.717 05	0.701 68	0.691 28	0.687 19
2.7215	0.835 78	0.799 72	0.789 97	0.777 47	0.772 72	0.769 65
2.8028	0.903 10	0.880 72	0.875 04	0.872 49	0.869 49	0.868 40
2.8840	0.974 07	0.967 90	0.970 42	0.972 82	0.977 32	0.978 20
2.9652	1.041 91	1.055 75	1.065 19	1.071 33	1.080 96	1.081 86
3.0465	1.098 64	1.131 05	1.145 71	1.157 08	1.168 36	1.174 05
3.1277	1.140 03	1.183 22	1.204 01	1.216 22	1.232 81	1.242 84
3.2090	1.158 27	1.209 02	1.230 33	1.245 29	1.263 77	1.276 03
3.2902	1.154 40	1.205 39	1.224 77	1.242 32	1.257 71	1.270 80
3.3714	1.133 13	1.177 49	1.192 25	1.207 71	1.220 21	1.228 03
3.4527	1.100 64	1.129 40	1.139 57	1.152 72	1.161 64	1.161 77
3.5339	1.062 33	1.075 23	1.077 02	1.086 72	1.088 19	1.087 20
3.6151	1.020 69	1.018 89	1.016 34	1.018 22	1.013 24	1.010 43
3.6964	0.984 98	0.969 26	0.961 96	0.954 49	0.947 43	0.943 20
3.7776	0.953 36	0.929 39	0.918 11	0.906 99	0.895 54	0.887 75
3.8589	0.933 00	0.903 15	0.890 61	0.874 42	0.861 22	0.851 72

TABLE III. (Continued.)

Γ	80	110	125	140	150	160
3.9401	0.921 72	0.888 49	0.875 14	0.859 87	0.845 50	0.839 06
4.0213	0.921 56	0.888 60	0.875 10	0.860 95	0.847 77	0.842 54
4.1026	0.929 09	0.902 25	0.891 13	0.880 78	0.868 19	0.865 44
4.1838	0.947 01	0.931 50	0.922 84	0.918 30	0.908 34	0.907 29
4.2651	0.971 48	0.962 87	0.961 27	0.962 76	0.956 93	0.961 39
4.3463	0.994 44	0.995 60	1.001 24	1.006 38	1.008 68	1.015 79
4.4275	1.013 48	1.025 35	1.036 83	1.041 62	1.052 01	1.059 45
4.5088	1.028 66	1.047 16	1.061 53	1.068 01	1.082 86	1.089 69
4.5900	1.038 64	1.061 18	1.074 60	1.081 54	1.099 98	1.101 24
4.6713	1.042 34	1.067 87	1.076 64	1.083 95	1.102 09	1.097 11
4.7525	1.039 51	1.066 32	1.071 61	1.077 30	1.090 63	1.085 81
4.8337	1.034 71	1.055 18	1.058 98	1.063 95	1.073 95	1.069 93
4.9150	1.029 51	1.042 28	1.038 82	1.047 56	1.050 94	1.045 96
4.9962	1.020 24	1.026 84	1.019 02	1.027 95	1.028 11	1.024 92
5.0775	1.006 37	1.008 97	0.999 66	1.008 04	1.001 18	1.001 93
5.1587	0.996 49	0.990 44	0.982 40	0.988 23	0.978 69	0.980 28
5.2399	0.986 68	0.973 48	0.971 50	0.971 31	0.960 04	0.967 34
5.3212	0.980 57	0.961 39	0.962 58	0.958 33	0.946 87	0.952 61
5.4024	0.976 63	0.953 64	0.957 60	0.946 57	0.938 01	0.947 44
5.4837	0.974 74	0.952 45	0.955 65	0.945 11	0.935 71	0.944 12
5.5649	0.975 38	0.956 26	0.960 67	0.945 79	0.936 38	0.950 07
5.6461	0.977 65	0.966 84	0.970 64	0.952 96	0.947 12	0.961 40
5.7274	0.984 90	0.982 21	0.985 81	0.967 98	0.967 90	0.968 50
5.8086	0.992 47	1.001 21	1.003 71	0.988 83	0.992 13	0.981 87
5.8898	1.007 04	1.021 13	1.018 20	1.008 36	1.017 00	0.996 51
5.9711	1.016 56	1.031 88	1.030 84	1.031 35	1.040 01	1.022 03
6.0523	1.022 49	1.045 42	1.036 97	1.050 50	1.068 27	1.040 14
6.1336	1.030 81	1.046 75	1.035 69	1.061 42	1.084 33	1.050 42
6.2148	1.029 64	1.039 56	1.024 64	1.063 99	1.083 33	1.050 93
6.2960	1.021 01	1.019 02	1.014 57	1.046 07	1.071 68	1.049 02
6.3773	1.007 36	1.014 06	1.009 06	1.021 64	1.048 00	1.035 31
6.4585	0.995 48	0.999 30	1.006 86	0.987 63	1.007 06	1.013 99
6.5398	0.988 87	0.993 61	0.993 49	0.969 39	0.967 62	0.997 14
6.6210	0.978 59	0.984 44	0.989 51	0.959 13	0.924 46	0.985 83
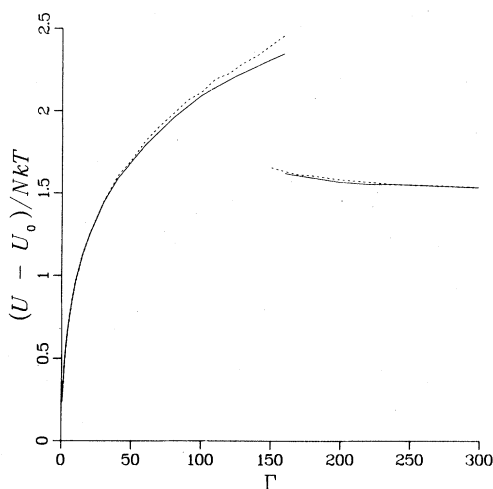
FIG. 2. Thermal fractions of internal energy (compared with a bcc lattice $U_0 = -0.895\,929\,256\,\Gamma$). Solid-curve data from this paper, dashed-curve data from Hansen (Ref. 2) and Pollock and Hansen (Ref. 10).

TABLE IV. Fitted liquid data for $1 \leq \Gamma \leq 160$. $U/NkT = a\Gamma + b\Gamma^{1/4} + c\Gamma^{-1/4} + d$, where $a = -0.897\,52$, $b = 0.945\,44$, $c = 0.179\,54$, and $d = -0.800\,49$.

Γ	U/NkT MC	U/NkT fitted	Relative error	Absolute error
1.0	−0.573	−0.573	0.000 03	0.000
2.0	−1.320	−1.320	−0.000 12	0.000
3.0	−2.112	−2.112	−0.000 14	0.000
4.0	−2.927	−2.927	0.000 22	−0.001
6.0	−4.593	−4.591	0.000 36	−0.002
10.0	−7.992	−7.994	−0.000 13	0.001
15.0	−12.309	−12.311	−0.000 22	0.003
20.0	−16.668	−16.667	0.000 07	−0.001
30.0	−25.431	−25.437	−0.000 21	0.005
40.0	−34.248	−34.252	−0.000 13	0.005
60.0	−51.961	−51.956	0.000 10	−0.005
80.0	−69.715	−69.715	0.000 01	0.000
100.0	−87.500	−87.506	−0.000 07	0.006
110.0	−96.411	−96.410	0.000 01	−0.001
125.0	−109.780	−109.775	0.000 04	−0.005
140.0	−123.157	−123.149	0.000 06	−0.008
150.0	−132.078	−132.068	0.000 07	−0.010
160.0	−141.000	−140.991	0.000 07	−0.009

TABLE V. U/NkT for $\Gamma \leqslant 1$.

Calculation Γ	Monte Carlo (MC)[a] calculated here	HNC (Ref. 9)	BSC (Ref. 8)	Abe (Refs. 6 and 2)	Hansen (Ref. 2) MC
0.1		−0.025·80	−0.0258	−0.025 90[b]	
0.2		−0.069 03[b]	−0.0688	−0.071 8	
0.3	−0.1225	−0.119 5[b]			
0.4	−0.1784	−0.177 3[b]			
0.5	−0.2383	−0.236 0[b]			
0.6	−0.3018[b]	−0.301 5			
0.7	−0.3668[b]	−0.364 4			
0.8	−0.4337[b]	−0.431 6			
0.9	−0.5035[b]	−0.500 4			
1.0	−0.573[b]		−0.577	−1.968	−0.580

[a]All values are the result of 10^6 configurations.
[b]Values used to calculate $F(\Gamma_1)/NkT$ numerically. The Abe analytic cluster expansion was used for $0 \leqslant \Gamma \leqslant 0.1$.

the relative and absolute errors of the fit and the values of the parameters. The fit to this form is extremely good; the relative rms error is 3×10^{-5}. A suggestive argument is presented by DeWitt and Rosenfeld[6] for the form of Eq. (5).

To find the liquid equation of state we calculate the Helmholtz free energy from the formula

$$\frac{F(\Gamma)}{NkT} = \int_0^\Gamma \frac{U}{NkT} \frac{d\Gamma'}{\Gamma'} \ .$$

Substituting for U/NkT from Eq. (5) we find

$$\frac{F(\Gamma)}{NkT} = a\Gamma + 4\left(b\Gamma^{1/4} - \frac{C}{\Gamma^{1/4}}\right) + d\ln\Gamma$$

$$- [a + 4(b - c)] + \frac{F(\Gamma_1)}{NkT} \ , \qquad (6)$$

where $F(\Gamma_1)/NkT$ is the free energy at $\Gamma = 1$. $F(\Gamma_1)/NkT$ was calculated by summing the results from a Simpson's rule integration of the starred values of U/NkT given in Table V ($0.1 \leqslant \Gamma \leqslant 1.0$) and an analytic integration of the Abe cluster[7] expansion formula [Eq. (19), Ref. 2] for U/NkT ($0.0 \leqslant \Gamma \leqslant 0.1$). The Abe formula was chosen for the lower end because it agrees well with the U/NkT values given by Broyles, Sahlin, and Carley[8] and by the hypernetted chain (HNC) approximation.[9] The HNC values were used in the integration for $\Gamma = 0.1$, 0.2, 0.3, 0.4, and 0.5. At $\Gamma = 0.6$ the HNC U/NkT agrees very well with the MC U/NkT consequently the MC values were used in the integration for $0.6 \leqslant \Gamma \leqslant 1.0$. The integration gives the result $F(\Gamma_1)/NkT = -0.420$. We consider this result to be more accurate than the corresponding Hansen[2] value $[F_{\text{Hansen}}(\Gamma_1)/NkT = -0.445]$ since a much denser grid was used for the integration and the U/NkT values are more accurate. [Note that $F(\Gamma_1)/NkT$ in Hansen's paper includes the perfect gas contribution.]

After including the perfect gas contribution [Eq.

(23), Ref. 2] Eq. (6) becomes

$$F(\Gamma)/NkT = a\Gamma + 4(b\Gamma^{1/4} - c/\Gamma^{1/4})$$

$$+ (d + 3)\ln\Gamma - [a + 4(b - c) + 1.135] \ . \qquad (7)$$

This formula for the liquid free energy may be used to calculate other thermodynamic variables of interest. We will use it shortly, after we have calculated the solid free energy, to find Γ at the liquid-solid transition (Γ_m).

Following Pollock and Hansen[10] we fit our 128-ion bcc lattice data to the form

$$\frac{U}{NkT} = \frac{U_0}{NkT} + \frac{3}{2} + \frac{h}{\Gamma^2} \ , \qquad (8)$$

by minimizing the squares of the relative errors. For the bcc lattice, $U_0/NkT = -0.895\,929\,\Gamma$. The fitted U/NkT are shown in Table VI along with the relative and absolute errors of the fit and the value of the parameter h. To obtain the Helmholtz free energy we use the harmonic approximation results from Ref. 10. This leads to

$$\frac{F}{NkT} = -0.895\,929\,256\Gamma + \tfrac{9}{2}\ln\Gamma - 1.8856 - \frac{h}{2\Gamma^2} \ . \qquad (9)$$

Since we now have formulas for the free energy

TABLE VI. Fitted solid data for $160 \leqslant \Gamma \; 300$. $U/NkT = 1.5 + U_0 + h/\Gamma^2$ where $U_0 = -0.895\,929\,\Gamma$ and $h = 2980$.

Γ	U/NkT MC	U/NkT fitted	Relative error	Absolute error
160.0	−141.729	−141.732	−0.000 02	0.003
170.0	−150.703	−150.705	−0.000 01	0.002
180.0	−159.675	−159.675	0.000 00	0.000
200.0	−177.619	−177.611	0.000 04	−0.008
220.0	−195.551	−195.543	0.000 04	−0.008
240.0	−213.469	−213.471	−0.000 01	0.002
300.0	−267.243	−267.246	−0.000 01	0.003

of both the liquid [Eq. (7)] and solid [Eq. (9)] we are now in a position to find the intersection of the two curves which gives the fluid-solid transition. We find that $\Gamma_m = 168 \pm 4$. The error in Γ_m was calculated by systematically biasing the U/NkT data (Table II) by $\pm \sigma_i$. The error of ± 4 corresponds the maximum and minimum intersection points of the three liquid free-energy curves (obtained by fitting $U_i/NkT - \sigma_i$, U_i/NkT, and $U_i/NkT + \sigma_i$) with the corresponding three solid free-energy curves.

Our results for $\Gamma_m = 168 \pm 4$ may be compared with the value of Pollock and Hansen,[10] $\Gamma_m = 155 \pm 10$. Again the difference is attributed to the relatively large systematic error in Hansen's[2] liquid data (Fig. 2). We note here that Van Horn's[11] estimate of $\Gamma_m = 170 \pm 10$ (based on the Lindeman melting criterion, harmonic theory, and empirical data) is in agreement with our more exact result.

IV. CONCLUSION

Using a very accurate representation of the Ewald potential and a Monte Carlo technique we have evaluated the internal energy of the classical one-component plasma ($1 \leqslant \Gamma \leqslant 300$). The liquid internal-energy data were fitted to a simple four-parameter equation which was then integrated to obtain the Helmholtz free energy of the system. After fitting the lattice internal-energy data to a one-parameter formula, and obtaining the solid free energy, we find that the fluid-solid transition is at $\Gamma = 168 \pm 4$.

Note added in proof. Subsequent calculations with $N = 250$, 432, and 686 have shown a dependence of U/NkT on N for values of Γ just below melting. The most recent Γ_m using the new results is $\Gamma_m = 171 \pm 3$.

APPENDIX A: CUBIC HARMONIC POTENTIAL APPROXIMATION

In this Appendix we discuss the form of the potential approximation following Slater and De-Cicco.[5] For a system of point charges surrounded by a uniform background charge, we expect the potential energy of a point charge to be given by

the sum of a solution to Poisson's equation for the uniform background [Eq. (A1)] and another solution for the point charges [Eq. (A2)].

First, for the potential of the uniform negative background, we need the solution to Poisson's equation $\nabla^2 \phi = -4\pi\rho$ in spherical coordinates. In this case the charge density ρ is $-Ze$. This leads to the solution $\phi = 2\pi r^2 Ze$ and thus the potential energy per NKT may be written as

$$\frac{W_1}{NkT} = \frac{(Ze)^2}{NkT} \phi = \frac{\Gamma}{NL} \frac{2}{3}\pi r^2 , \tag{A1}$$

since $\bar{r}L \equiv 1$. A term of this form did not appear in Hansen's approximation.

Next, we anticipate that the solution to Poisson's equation with cubic symmetry for the point charges is given by the expression

$$\frac{W_2}{NkT} = \lim_{r \to 0} \frac{\Gamma}{NL} [u_1(r) + 1 + u_2(r)]$$
$$+ \frac{\Gamma}{NL} \text{(fitted cubic harmonics)} ,$$

which in the limit goes to

$$\frac{W_2}{NkT} = \frac{\Gamma}{NL} \left(\frac{1}{r} + 1 - E_m \right)$$
$$+ \frac{\Gamma}{NL} \text{(fitted cubic harmonics)} . \tag{A2}$$

The fitting parameters in the cubic harmonics remain to be determined.

We digress for a few comments about the cubic harmonics. Explicitly we used cubic harmonic polynomials in the coordinates l, m, and n where $l = x/r$, $m = y/r$, and $n = z/r$, and x, y, and z are the usual Cartesian coordinates.

Examples of the first 3 normalized functions follow:

$$K_2 = P_2(l) + P_2(m) + P_2(n) = 0 ,$$
$$K_4 = V_1' r^4 [P_4(l) + P_4(m) + P_4(n)]$$
$$= V_1 r^4 (l^4 + m^4 + n^4 - \tfrac{3}{5}) ,$$
$$K_6 = V_2' r^6 [P_6(l) + P_6(m) + P_6(n)]$$
$$= V_2 r^6 [l^6 + m^6 + n^6$$
$$- \tfrac{15}{11}(l^4 + m^4 + n^4) + \tfrac{30}{77}] ,$$

where $P_i(l)$ are the usual Legendre polynomials and the V_i's are the fitted constants (the V_i''s differ by a constant factor).

To obtain the required accuracy we used terms through K_{22}. Terms of degree 12, 16, 18, 20, and 22 are degenerate and consequently each needs an orthogonal function of the same degree to complete the basis set. We used only the 12th degree function,

$$\overline{K}_{12} = V_{11} \mathrm{Re}[(l + im)^{12} + (m + in)^{12} + (n + il)^{12}] \, ,$$

where the V_{11} is fitted along with V_1 (for K_4) through V_{10} (for K_{22}).

Adding Eqs. (A1) and (A2) we obtain for the potential between two particles with separating distance $r = (x^2 + y^2 + z^2)^{1/2}$,

$$\frac{\psi}{NKT} = \frac{\Gamma}{NL} \left(\frac{1}{r} + C_0 + C_2 r^2 + V_1 r^4 (S_4 + C_{4,1}) \right.$$

$$+ V_2 r^6 (S_6 + C_{6,1} S_4 + C_{6,2})$$

$$\cdot$$
$$\cdot$$
$$\cdot$$

$$+ V_{10} r^{22} (S_{22} + C_{22,1} S_{20} + C_{22,2} S_{18} + \cdots$$

$$\left. + C_{22,9} S_4 + C_{22,10}) + V_{11} \overline{K}_{12} \right) ,$$

where $C_0 = 1 - E_m$, $C_2 = 2\pi/3$, $S_j = (x^j + y^j + z^j)/r^j$, and the C_{ji} are the collected Legendre coefficients

For computational convenience this expression is rearranged by collecting like powers of r^2. Letting $T_j = S_j r^j = x^j + y^j + z^j$, $U_j = V_{(j-2)/2}$, and $U_2 = C_2$ we have

$$\frac{\psi}{NKT} = \frac{\Gamma}{NL} \left(\frac{1}{r} + C_0 \right.$$

$$+ T_2(U_2 + C_{4,1} U_4 r^2 + C_{6,2} U_6 r^4 + C_{8,3} U_8 r^6$$

$$+ \cdots + C_{22,10} U_{22} r^{20})$$

$$+ T_4(U_4 + C_{6,1} U_6 r^2 + C_{8,2} U_8 r^4 + C_{10,3} U_{10} r^6$$

$$+ \cdots + C_{22,9} U_{11} r^{18})$$

$$\cdot$$
$$\cdot$$
$$\cdot$$

$$+ T_{20}(U_{20} + C_{22,1} U_{22} r^2)$$

$$+ T_{22} U_{22}$$

$$\left. + U_{24} \overline{K}_{12} \right) . \qquad (A3)$$

The coefficients for the r^2 terms (e.g., $C_{4,1} U_4$ and $C_{22,1} U_{22}$) are calculated once and placed in a matrix (A_{ji}) which is subsequently used in calculating the coefficients for the T_j's.

To calculate the potential given the separation x, y, and z we first compute the T_j coefficient as polynomials in r^2 using A_{ji}. Since the T_j's are simply polynomials in x^2, y^2, and z^2 we next calculate each x^2, y^2, and z^2 polynomial using the T_j coefficients. These results are then added to the left-over terms $(1/r + C_0 + U_{24} \overline{K}_{12})$ for the final result.

A table of 8000 values of the function ψ/NkT

[Eqs. (2), (3), and (4) were generated. These values were approximated by the function ψ/NkT in Eq. (A3) by adjusting the parameters V_1, V_2, ... so as to minimize the mean-square error. Note that Eq. (A3) does not require evaluation of the error function complement.

APPENDIX B: EXTENSION OF THE RANGE OF THE PAIR DISTRIBUTION FUNCTIONS FOR SPHERICALLY SYMMETRIC DISTRIBUTIONS

In a Monte Carlo calculation, for each configuration the pair separations are computed between a particle under consideration and all others whose x, y, and z coordinates are within half of the periodic distance. The number of particles within an interval at a certain distance, say $a \pm d$ where d is small radial increment, are accumulated into a bin. At the end of the calculation the number in the bin is divided by the volume of the bin at that distance times the number of configurations to get the pair distribution function for that bin. Although all pair separations are calculated within a box of side L centered on a particle, pair distributions are usually only tabulated for pairs in a sphere of diameter L centered on the particle. About half of the pairs in the box are outside the sphere. We show here a method for using the pairs which are usually neglected. For spherically symmetric distributions, this method will extend the pair distribution function from $\frac{1}{2}$ to $\sqrt{\frac{3}{2}}$ where the length of the edge of the basic cube is taken as 1. For distributions without spherical symmetry, the following procedure provides a method for determining the deviation from spherical symmetry.

Consider a sphere of radius a centered in a cube with edge length 1. For a spherical shell with radial increment d, the volume is given by the expression $V_1(a, d) = V_V(a) - S_V(a - d)$ where $S_V(a) =$
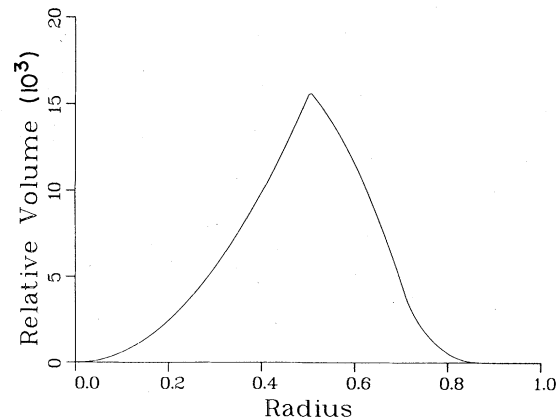
FIG. 3. Normalizing volume for the pair distribution functions.

$\frac{4}{3}\pi a^3$. As the shell grows outwards, the outer sphere becomes tangent to the six faces of the cube at $a = \frac{1}{2}$. For $a > \frac{1}{2}$ and before the outer sphere is tangent to the edges of the cube, at $a = \sqrt{2}/2$, the volume of the shells must be diminished by the volume of the "caps" protruding beyond the faces of the cube. The volume of the shells in this region are given by the formula: $V_2(a, d) = V_1(a, d) - [C_V(a) - C_V(a-d)]$, where $C_V(a) = 2\pi(a - \frac{1}{2})^2(2a + \frac{1}{2})$. For $\sqrt{2}/2 < a < \sqrt{3}/2$ the caps overlap at the edges of the cube and the shell volume is diminished unnecessarily by the volume in the 12 overlaps. The volume of the shells in this overlap region may be expressed as

$$V_3(a, d) = V_2(a, d) + [O(a) - O(a - d)]$$

where

$$O(a) = (12a^2 - 1)\{\sin^{-1}\tfrac{1}{2}/[(a^2 - \tfrac{1}{4})^{1/2}] - \tfrac{1}{2}\pi\}$$
$$+ 16a^3 \sin^{-1}\{(a^2 - \tfrac{1}{2})^{1/2}/[2(a^2 - \tfrac{1}{4})]^{1/2}\}$$
$$+ 2(a^2 - \tfrac{1}{2})^{1/2}.$$

Figure 3 shows the relative volumes of the shells out to $a = \sqrt{3}/2$. The smaller volumes near $\sqrt{3}/2$ (where the spherical shells are near the vertices of the cube) indicate decreasing accuracy in the statistics for the pair distribution functions in this region.

[1]S. G. Brush, H. L. Sahlin, and E. Teller, J. Chem. Phys. **45**, 2102 (1966).

[2]J. P. Hansen, Phys. Rev. A **8**, 3096 (1973).

[3]H. E. DeWitt, Phys. Rev. A **14**, 1290 (1976).

[4]H. E. DeWitt and W. B. Hubbard, Astrophys. J. **205**, 295 (1976).

[5]J. C. Slater and P. DeCicco, MIT Solid State and Molecular Theory Group Quarterly Progress Report No. **50**, 46 (1963).

[6]H. E. DeWitt and Y. Rosenfeld, Phys. Lett. (in press).

[7]R. Abe, Prog. Theor. Phys. **22**, 213 (1959).

[8]A. A. Broyles, H. L. Sahlin, and D. D. Carley, Phys. Rev. Lett. **10**, 319 (1963).

[9]Calculated by the method of K-C. Ng, J. Chem. Phys. **61**, 2680 (1974).

[10]E. L. Pollock and J. P. Hansen, Phys. Rev. A **8**, 3110 (1973).

[11]H. M. Van Horn, Phys. Lett. **28A**, 707 (1969).